Journal of Magnetic Resonance **136,** 54–62 (1999)
Article ID jmre.1998.1622, available online at http://www.idealibrary.com on IDEAL®

Composite Pulsed Field Gradients with Refocused Chemical Shifts and Short Recovery Time

Haitao Hu and A. J. Shaka[1]

Chemistry Department, University of California, Irvine, California 92697-2025

Received May 28, 1998; revised September 15, 1998

An improved self-compensating pulsed field gradient (PFG) technique that combines antiphase gradient pairs with broadband frequency-modulated 180° pulses is proposed. The antiphase gradient pairs lead to superb system recovery. In addition, evolution under chemical shift and heteronuclear *J* coupling are refocused during the PFG, making it appear effectively instantaneous. This new approach makes it possible to obtain high-resolution *phase-sensitive* 2D spectra for the PFG version of many experiments such as COSY, DQF-COSY, and HSQC without adding extra compensating delays or pulses. While reasonable suppression of unwanted magnetization is achieved, this method also gives satisfactory retention of desired signals. As a bonus, the field-frequency lock is not perturbed during the experiments. © 1999 Academic Press

Key Words: **pulsed field gradient; frequency-modulated pulse; phase-sensitive 2D NMR spectra; PFG DQF-COSY; PFG HSQC; lineshape.**

INTRODUCTION

The pulsed field gradient (PFG) has been proven to be one of the most useful tools in modern NMR experiments, so that numerous new methods are based on it. One widely used application of PFGs is to dephase unwanted transverse magnetization, as in solvent suppression, using so-called crusher gradients (*1–3*). Various solvent suppression methods have been developed in the past decade, among which several of the most successful rely on the use of gradients (*4–7*). A recent breakthrough is the excitation sculpting technique using a double pulsed field gradient spin echo (DPFGSE) (*8*), in which very high suppression ratios can be achieved while the phase of the spectrum remains well behaved. The DPFGSE has achieved success in other NMR experiments (*9–12*) as well.

Pulsed field gradients are also commonly used to improve artifact suppression, thereby giving "cleaner" spectra. While artifacts caused by fast pulsing and pulse imperfections can be attenuated by phase cycling (*13–15*), the minimum experiment time inevitably lengthens. For example, to suppress artifacts associated with 180° pulse imperfections in a spin echo sequence, τ–180°–τ, the EXORCYCLE phase cycling scheme (*13*) can be implemented with a four-step phase cycle. For a pulse sequence with n such components, independent EXORCYCLE phase cycling of the n 180° pulses would require 4^n steps, which soon becomes impractical with the increase of n. However, it is well known that the same degree of suppression can be achieved in *a single transient* using the pulsed field gradient spin echo (PFGSE) G–180°–G (*16*). This is, in fact, a simple example of coherence transfer pathway selection (*17, 18*) using gradients (*19–23*). The fundamental principle underlying this technique is that the rate of dephasing of a coherence in an inhomogeneous magnetic field is proportional to its coherence order (*19, 20, 24*). This allows selection of a particular coherence transfer pathway in *a single transient* regardless of the coherence order (*20, 21*), while in the phase-cycled multiple-quantum-filtered COSY experiment (*25, 26*), for instance, it would require at least four transients to select double-quantum coherence and even more transients for selective detection of higher order coherences (*18, 26*). Furthermore, solvent suppression and artifact suppression are often accomplished in conjunction with coherence transfer pathway selection when gradients are used, as the solvent resonance and artifacts experience different pathways from the desired magnetization and thus are dephased by the gradients together with other unwanted signals (*20–23, 27, 28*).

Conventional PFGs have, however, several problems. First of all, the application of an intense PFG induces eddy currents that may last for periods up to a millisecond or so even on an actively shielded gradient coil, meaning that recovery delays of at least the same order must be added after the gradient to allow the magnetic field to reestablish stability and homogeneity. Some signal loss can result if the relaxation time of the sample molecule is short, as is often true in protein studies. Improvements in probe design can, of course, minimize the recovery time but they cannot address a related problem: gradients are not instantaneous. Depending on the situation, gradient durations from 200 μs to 1 ms are commonly used. Chemical shift and spin–spin coupling will keep evolving throughout the gradient and any necessary recovery delay that follows, presenting great difficulties to the correct phasing of the final spectra of many PFG experiments. In the 2D case it is even more problematic to phase the spectrum correctly if uncompensated long delays are present in both t_1 and t_2, such as in

[1] To whom correspondence should be addressed. E-mail: ajshaka@uci.edu.

1090-7807/99 $30.00

the PFG COSY experiment (*21*). As a result, the spectra of routine 2D PFG experiments are presented in absolute-value mode, while the resolution and extra information contained in the phase properties are sacrificed. Finally, a conventional gradient perturbs the field-frequency lock. Even though this does not seem to cause any major deleterious effects in most situations, it would still be preferable to avoid it to maintain the best possible field/frequency regulation and shimming over time.

We propose to dispense with these problems by fabricating a more ideal PFG along the same lines as composite RF pulses. We combine several PFGs together with some RF pulses so that the net effect is an instantaneous nucleus-selective PFG with essentially zero recovery time. The resulting composite PFG can be used in a wide variety of experiments, and can oftentimes be blindly substituted for a conventional PFG without any further thought. It could thus be coded into a software subroutine and then used to update existing pulse sequences.

THEORY

An Ideal PFG

As in the area of composite 180° pulses, we can make up for instrumental limitations like finite gradient amplitude and nonzero recovery time by combining PFGs with radiofrequency (RF) pulses. Just as an ideal inversion pulse should map $I_z \rightarrow -I_z$ independently of resonance offset or RF inhomogeneity, our goal here is to seek an ideal PFG (*29*). Such an ideal PFG will *instantaneously wind all transverse magnetization of a selected spin species into a perfect helix of specified pitch along the gradient axis, with zero recovery time needed after the application of the gradient pulse, leaving z magnetization unaffected.* The suppression ratio depends on *all* transverse magnetization being dephased, the specificity is important for some realizations of "joint" experiments, the instantaneous criterion allows no time for evolution under chemical shift or spin–spin coupling, and the zero recovery time allows either data acquisition or further pulses to be applied immediately following the ideal PFG. We will see how closely the ideal PFG can be approached using imperfect RF pulses and conventional PFGs.

Compensated PFGs

Figure 1 shows some timing diagrams for several combinations of RF pulses and PFGs. The most commonly used technique to try to fix the phasing problem stated above is by introducing a conventional 180° pulse and a compensating delay (*27*), as shown in Fig. 1b. Evidently, the signal loss due to relaxation will get worse as this sequence necessarily takes longer. In addition, this scheme may also lead to artifacts in the spectrum and cause the retention of desired signals off resonance to suffer due to imperfections intrinsic to the conventional 180° pulse. On the other hand, suppression of transverse magnetization remains perfect, and chemical shifts are refocused if the timing is correct. Note that reversing the time line in Fig. 1b and attempting to place the 180° pulse after the PFG,

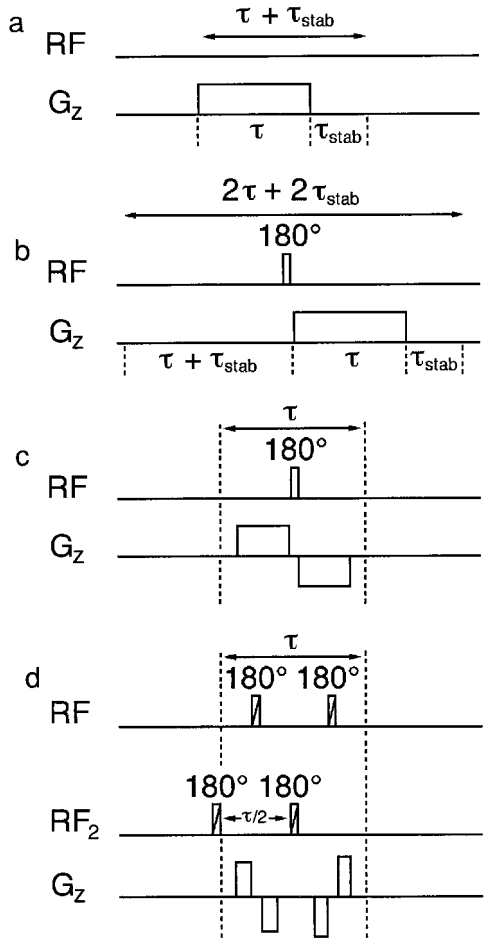

FIG. 1. Four different pulsed field gradient sequences. (a) A gradient of length τ is followed by a stabilization delay τ_{stab}. Typical values might be 1 ms and 250 μs, respectively. Chemical shifts and spin–spin couplings will evolve throughout this time. (b) A conventional 180° pulse together with a compensating delay can be introduced to refocus evolution under chemical shift and heteronuclear spin–spin couplings. The sequence becomes twice as long and the 180° pulse may give rise to artifacts and cause signal loss off resonance. (c) The scheme proposed by Wider *et al.* in which the 180° pulse is placed within the gradient and half of the gradient pulse is applied with opposite polarity. The stabilization time τ_{stab} becomes negligible with this arrangement, but suppression of unwanted transverse magnetization is degraded. (d) The "double-decker sandwich" scheme proposed in this work. We propose the acronym *c*omposite gradient *l*eaving an *u*ndisturbed B_0 field (CLUB) for this approach. Two high-power, constant-amplitude frequency-modulated pulses (shown as the scored icons) with superior inversion performance are applied between *two* sets of antiphase gradients with unequal durations or/and strengths. The total effective gradient intensity is simply the sum of those of all four gradients. Suppression of unwanted magnetization is substantially improved, as is retention of desired signals. The poor phase properties of the inversion pulses have no effect on the performance because of the inherent double spin echo nature. Optionally, a second set of FM 180° pulses can be applied (shown as RF_2) as shown to refocus transverse magnetization from other spins: in the case shown there is no phase encoding, but by offsetting these pulses differently and breaking each gradient up into two PFGs, variable encoding on different nuclei can be achieved.

so as to fold some of the eddy current recovery time into the compensating delay, will not suppress any transverse magnetization *created* from z magnetization by the 180° pulse itself, and so can lead to poor suppression. Figure 1c shows an improved modification introduced by Wider *et al.* (*30*) in which the conventional PFG is replaced by a pair of matched antiphase PFGs centered around a conventional 180° pulse, a unit we will call a "PFG sandwich." This arrangement substantially improves the recovery (*30*) as the eddy currents induced by the two juxtaposed opposite polarity PFGs nearly cancel. For the part of magnetization which gets inverted by the 180° pulse, evolution under chemical shift and heteronuclear J coupling are refocused, as was first demonstrated by Wider *et al.* in a phase-sensitive 2D PFG NOESY experiment (*31*). Homonuclear J coupling will still evolve, but in practical applications $J\tau_g \ll 1$ for proton couplings $J \sim 10$ Hz and PFG times $\tau_g \sim 1$ ms and thus can be neglected. Another interesting point here is that the use of RF pulses also makes the PFG sandwich nucleus-selective. This should be obvious because other nuclear species just experience two antiphase PFGs of equal intensity whose effects cancel each other. As a result, the field-frequency lock is only momentarily perturbed since no RF pulses are applied to the deuterium lock channel. However, notice that the z magnetization of the "target" spins is inverted by this sequence, meaning that the latter cannot represent a true ideal gradient. One potential problem with this is radiation damping caused in the case of a large positive H_2O z magnetization which gets inverted (*32*). Other unexpected results may also arise when one tries to substitute this sequence for a conventional PFG. For instance, in the simple PFG spin echo experiment 90°–G–180°–G–, blindly substituting this scheme into the pulse sequence for G turns out to dephase the signal, while an echo is certainly expected! Aside from this, careful examination of the PFG sandwich shows that while the retention off resonance remains questionable due to the use of a conventional 180° pulse, suppression can also be substantially degraded. This observation is supported by both experiments and product operator analysis (*33, 34*). In an earlier treatment (*8*) of the PFGSE sequence G–S–G, where G is a sufficiently strong PFG and S is any arbitrary sequence of pulses that can be represented by the unitary transformation

$$U_s = \exp(-i\beta I_z)\exp(-i\theta I_y)\exp(-i\alpha I_x)\exp(i\theta I_y)\exp(i\beta I_z), \quad [1]$$

the transformation matrix from some arbitrary initial state $\sigma(0) = \mathbf{m} \cdot \mathbf{I}$ immediately preceding the PFGSE to the final state $\sigma(t) = \mathbf{M} \cdot \mathbf{I}$ was calculated for a single spin using the product operator formalism neglecting relaxation. The same algorithm can be applied to the PFG sandwich with some modifications. Let $\mathbf{m} = (m_x, m_y, m_z)$ be now the input vector of the PFG sandwich and $\mathbf{M} = (M_x, M_y, M_z)$ the output vector; the corresponding components of the two vectors are related by (*8*)

$$M_\alpha = \frac{1}{2\pi}\int_0^{2\pi} \mathrm{Tr}\{I_\alpha \exp(i\phi I_z) U_s \exp(-i\phi I_z) \times \sigma(0) \exp(i\phi I_z) U_s^\dagger \exp(-i\phi I_z)\}\, d\phi, \quad [2]$$

where $\alpha = x, y, z$. Equation [2] can be written in the compact form $\mathbf{M} = \mathbf{Tm}$, where $\mathbf{T}$ is a 3×3 matrix. Carrying out the integration over ϕ, we find

$$\mathbf{T} = \begin{bmatrix} \cos\alpha + P & \sin\alpha \sin\theta & 0 \\ -\sin\alpha \sin\theta & \cos\alpha + P & 0 \\ 0 & 0 & 1 - 2P \end{bmatrix} \quad [3]$$

for the PFG sandwich, where

$$P \equiv \frac{1}{2}\left(1 - \frac{M_z}{m_z}\right) = \frac{1}{2}(1 - \cos\alpha \cos^2\theta - \sin^2\theta) \equiv \cos^2\theta \sin^2(\alpha/2) \quad [4]$$

is the probability that a spin is flipped by the sequence S and satisfies $0 \le P \le 1$ (*35*). It is interesting to note the block diagonal structure of $\mathbf{T}$, similar to that obtained for the PFGSE, showing that transverse and longitudinal magnetization transform independently of each other. We now define the normalized intensity of the residual signal as

$$\eta \equiv \frac{|M_{\mathrm{trans}}|}{|m_{\mathrm{trans}}|} \equiv \frac{\sqrt{M_x^2 + M_y^2}}{\sqrt{m_x^2 + m_y^2}}, \quad [5]$$

where the subscript trans denotes transverse magnetization. Note that the suppression ratio is simply the inverse of η. After some simplification, we then find

$$\eta = \sqrt{(\cos\alpha + P)^2 + \sin^2\alpha \sin^2\theta} = \sqrt{(1 - P)^2} = 1 - P. \quad [6]$$

Equation [6] shows that a fraction $(1 - P)$ of the transverse magnetization "breaks through" the PFG sandwich with no phase encoding. Note that in the ideal case $P = 1$ Eq. [6] would give $\eta = 0$, corresponding to infinite suppression. An intuitive way to interpret this result is that the part of magnetization that does *not* get flipped by the inversion pulse is refocused by the second PFG of opposite polarity. Assuming that the individual gradients are strong, the net suppression of transverse magnetization achieved by the PFG sandwich depends solely on how well the sequence S inverts z magnetization. For a conventional 180° pulse the fraction $(1 - P)$ can be up to 10% off resonance depending on

the RF power available and the spatial homogeneity of the B_1 field over the detected sample volume, leading to modest suppression ratios on the order of 10–50 instead of the essentially infinite ratio achieved by a conventional gradient. For example, even a perfectly homogeneous 20-μs 180° pulse gives $P < 0.98$ for offsets $|2\pi\Delta\omega| > 3.5$ kHz, and hence a predicted suppression ratio of less than 50 outside this range of offsets.

Based on these observations, and experience with the DPFGSE, we propose the improved method shown in Fig. 1d which employs two PFG sandwiches with opposite sense. This "double-decker sandwich" is identical to the DPFGSE sequence, except that the polarity of the two gradients in the center is inverted. The layers in the sandwich have to be arranged so that transverse magnetization keeps dephasing throughout the sequence: the total effective gradient intensity is then simply the sum of all four gradients. We propose the acronym *c*omposite gradient *l*eaving an *u*ndisturbed B_0 field (CLUB) for the double-decker sandwich. The fast-recovering property of the PFG sandwich is preserved by this scheme, evolution under chemical shift and heteronuclear spin–spin coupling are refocused, and the application of two inversion pulses restores z magnetization to its prior state. The phase property of the inversion pulse does not matter because the use of two such identical pulses leads to no unwanted phase shifts where the inversion is excellent (*8*). We thus propose to use new broadband high-power constant-amplitude frequency-modulated (FM) pulses that we have designed to achieve $P \rightarrow 1$. Finally, the CLUB sandwich is also nucleus-selective: as mentioned earlier, spins not receiving the inversion pulses simply experience a pair of matched antiphase gradients, which amounts to a net delay for those other spins. In most cases, this delay will have no effect on the outcome of the experiment. If the spin system of interest is homonuclear then evolution of heteronuclei is irrelevant, and if the magnetization of those other nuclear species is along the z axis it will not evolve coherently during a delay, such as in the PFG HSQC experiment (*36, 37*). It is possible to compensate for this delay by inserting a pair of optional FM 180° pulses to these X nuclei as shown in Fig. 1d. Altering the position of the pulses allows for variable phase encoding of these other spins, so that they experience a given fraction of the net PFG. This may prove useful for the realization of some potential "joint" experiments in which both ^{1}H–^{13}C and ^{1}H–^{15}N 2D spectra are obtained simultaneously.

As in the analysis of the DPFGSE, we claim that the transformation matrix for the CLUB sandwich is simply $\mathbf{T}^2$ (*8*), $\mathbf{T}$ being given by Eq. [3]:

$$\mathbf{T}^2 = \begin{bmatrix} (\cos\alpha + P)^2 - \sin^2\alpha\sin^2\theta & 2(\cos\alpha + P)\sin\alpha\sin\theta & 0 \\ -2(\cos\alpha + P)\sin\alpha\sin\theta & (\cos\alpha + P)^2 - \sin^2\alpha\sin^2\theta & 0 \\ 0 & 0 & (1-2P)^2 \end{bmatrix}. \quad [7]$$

The only requirement for the validity of Eq. [7] is that the gradients used in the second sandwich be uncorrelated to those used in the first one (*8*) to avoid any accidental refocusing, which can be readily accomplished under computer control. We now proceed to calculate the normalized intensity of the residual signal after applying a CLUB sandwich:

$$\begin{aligned} \eta &= \sqrt{[(\cos\alpha + P)^2 - \sin^2\alpha\sin^2\theta]^2 + 4\sin^2\alpha\sin^2\theta(\cos\alpha + P)^2} \\ &= \sqrt{[(\cos\alpha + P)^2 + \sin^2\alpha\sin^2\theta]^2} \\ &= (1-P)^2. \end{aligned} \quad [8]$$

Equation [8] shows that the suppression has been greatly improved since now the fraction that "breaks through" becomes $(1-P)^2$ which is much less than $(1-P)$ when $P \rightarrow 1$. Once a high level of suppression is achieved, simple phase shifting of either FM inversion pulse by 90° combined with a receiver phase shift of 180° can make the suppression essentially infinite to the extent the spectrometer is stable. We next show that the CLUB sandwich can be served up in a variety of common PFG experiments.

EXPERIMENTAL

Recovery and Suppression Performance

To verify the previous predictions, we performed a few simple experiments. Figures 2a and 2b show the pulse sequences we used to study the suppression. Data were collected with one single scan on a 1% H_2O/99% D_2O sample (containing a small amount of $GdCl_3$ to bring the proton T_1 to ~250 ms). In both cases a conventional hard inversion pulse was used. In Fig. 2b the two sets of gradients had different durations for reasons described above. The duration of the inversion pulses was fixed at 20 μs while the RF power of the inversion pulses was systematically arrayed to achieve different values of P and the corresponding intensity of the residual signal was recorded. In one case the inversion pulses were literally "turned off" by shifting the transmitter way off resonance and setting the RF power to the lowest level available. This should give no suppression of the signal in question at all since $P = 0$ in this case, so this peak intensity can be used as the reference for normalization. All experiments described in this article were performed on a Varian UnityPlus 500-MHz spectrometer equipped with a 5-mm Varian triple-resonance

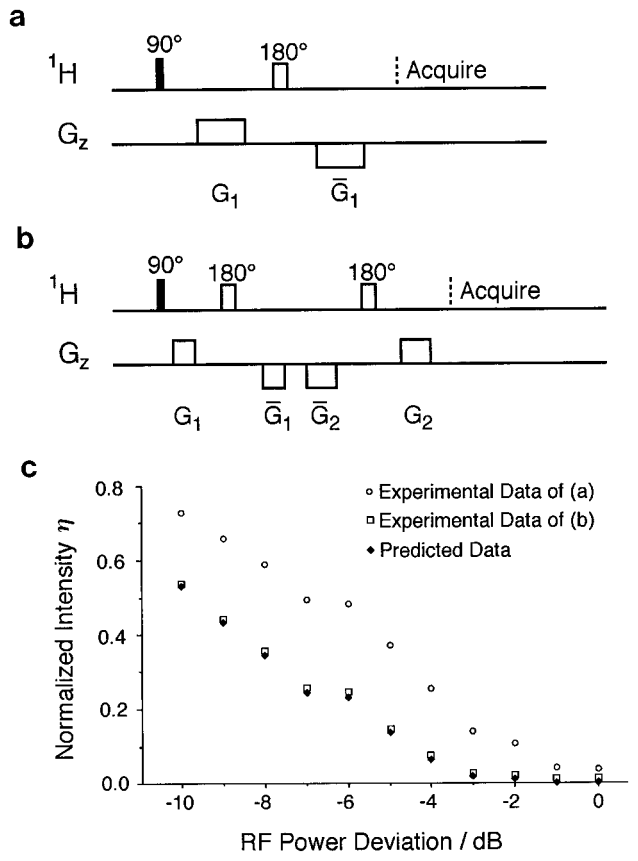

FIG. 2. Suppression study. (a) Using the PFG sandwich. (b) Using the CLUB sandwich scheme. The gradients used in (a) were 500 μs in duration with a strength of 5 G/cm, while those in (b) were 200 and 300 μs in duration, respectively, and applied at 10 G/cm. (c) The normalized intensity η of the residual signal as a function of the RF power of the inversion pulses in (a) and (b). In each case 11 different values were used for the RF power while the duration was fixed at 20 μs to achieve different values of P. Note that the horizontal axis is labeled as deviation from the nominal RF power required to give a 20-μs 180° pulse. Data obtained with the pulse sequence of (a) are represented by open circles, while those obtained using (b) are shown as open squares. The filled diamonds are the predicted data from Eq. [8], being simply the arithmetic squares of the open circles. All experimental data were collected with a single transient on a doped H_2O/D_2O sample.

PFG probe and waveform generator. All PFGs were along the z axis of the sample.

Figure 2c shows the experimental results obtained using the pulse sequences of Figs. 2a and 2b along with the predicted data from Eq. [8], the latter being simply squares of those obtained using the pulse sequence of Fig. 2a. The normalized intensity of the residual signal is plotted as a function of the RF power deviation from the nominal RF power required to give a 20-μs 180° pulse. Toward the right side of the horizontal axis it corresponds to smaller deviation and thus better inversion, or greater values of P. For relatively smaller values of P (<0.9), the experimental results match almost perfectly with the calculated data, showing that the suppression ratio does get squared as predicted by Eq. [8]. As P gets closer to unity, however, this requirement becomes so critical that other minor factors like spectrometer instability and the distribution of B_1 fields over the sample volume now play a crucial role in dictating the degree of suppression. In particular, if P is a function of space because of B_1 inhomogeneity, then some values of P may be low in regions that couple poorly to the receiver coil. This small percentage that is poorly inverted does not result in much percentage error except when the rest of the sample is nearly perfectly inverted, and the relevant inequality is

$$\int W(\mathbf{r})\,P(\mathbf{r})^2 d\mathbf{r} > \left[\int W(\mathbf{r})\,P(\mathbf{r})\,d\mathbf{r}\right]^2, \qquad [9]$$

where the nonnegative spatial weight function $W(\mathbf{r})$ describes the coupling of the spatial region to the receiver coil. Poor inversion of a small percentage of the sample can thus limit the observed improvement to a factor of 5–10 in practice instead of the predicted 10–50, which improves the suppression ratio from 10–50 to several hundred in this particular case.

However, further improvement can be achieved by replacing the conventional 180° pulses in Fig. 2b with broadband high-power FM pulses shown in Fig. 3. The maximum convenient RF field we can achieve on the ^{1}H channel is 25 kHz, corresponding to a 90° pulsewidth of 10 μs. The 60-μs duration of

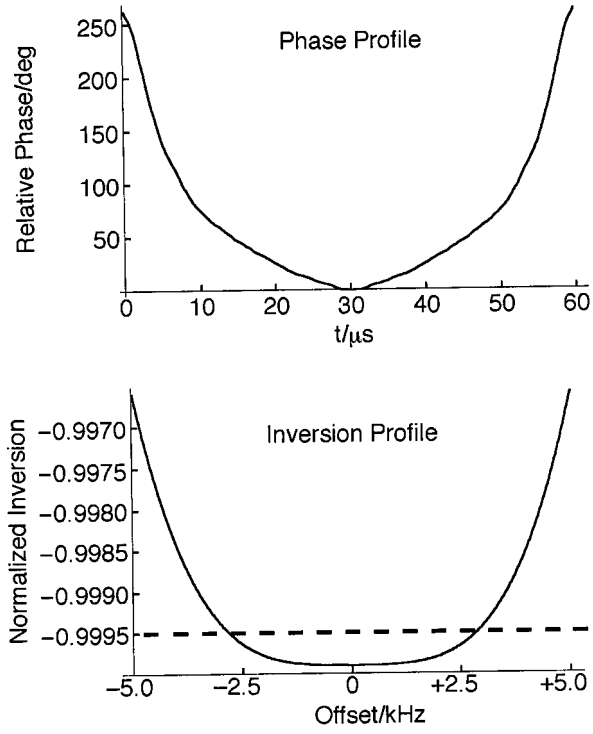

FIG. 3. The phase profile versus time and inversion profile versus frequency of a constant-amplitude FM pulse. Better than 99.99% inversion is achieved over a bandwidth of ±2.5 kHz using a 60-μs pulse applied at a 25-kHz RF field (10 μs 90°).

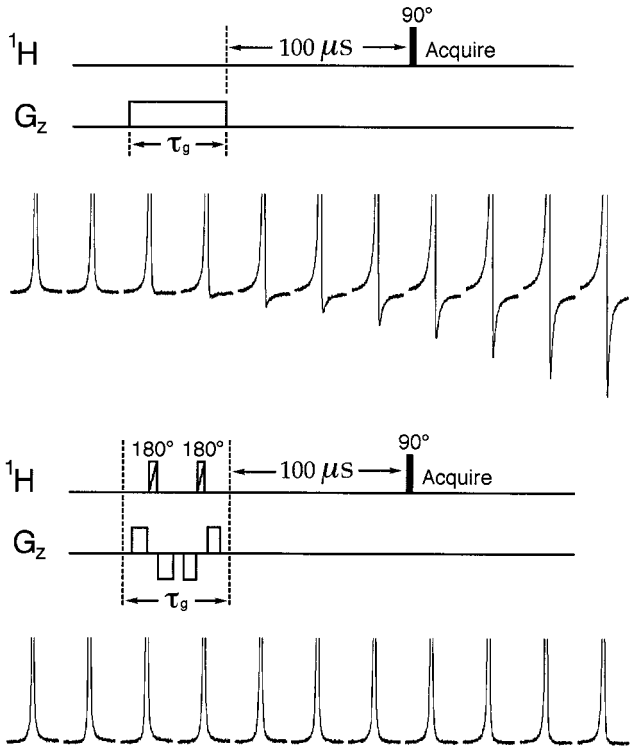

FIG. 4. Comparison of the recovery of a conventional gradient with that of the CLUB sandwich. The stabilization delay was fixed at 100 μs in both cases, while the gradient strength was incremented from 0 to 30 G/cm in 3 G/cm steps and the total effective duration of the gradient τ_g was fixed at 1 ms. Spectra were acquired with a single transient on a doped H_2O/D_2O sample. (Top) The response recorded using a conventional gradient. At very high gradient strength the phase is twisted and the Lorentzian lineshape is altered. (Bottom) The response obtained using a CLUB sandwich. The constant-amplitude FM pulse of Fig. 3 was used as the inversion element. The phase remains constant as the gradient strength is incremented, as does the Lorentzian lineshape. The recovery is clearly substantially less than 100 μs.

this constant-amplitude inversion pulse is relatively brief, and has been designed to achieve excellent inversion over the typical 10 ppm bandwidth of 5 kHz at 500 MHz for protons. The calculated extent of inversion is shown in Fig. 3 and is better than 99.99% over a bandwidth of ± 2.5 kHz, or 10 ppm on our spectrometer. There is also high tolerance for pulse miscalibration or RF inhomogeneity. With this better inversion pulse, suppression can be substantially improved. In practice suppression ratios on the order of 10^3 are observed.

Figure 4 compares the recovery of a conventional gradient with the CLUB sandwich approach. Spectra were acquired with one single scan on the same doped H_2O/D_2O sample. The recovery delay in both cases was fixed at 100 μs and the gradient duration at 1 ms. The gradient strength was then incremented from 0 to 30 G/cm in 3 G/cm steps. The upper trace shows the response of a conventional gradient. A closer look at the spectra reveals that at very high gradient strength not only is the phase affected, but the Lorentzian lineshape is also altered. The lower trace shows spectra obtained using the CLUB sandwich. Even at 30 G/cm the recovery is substantially less than 100 μs and the lineshape remains Lorentzian.

As pointed out earlier, even though the phase-sensitive mode gives better resolution and allows interpretation of the extra information that might be contained in the phase properties of the spectra, the use of conventional gradients often leads to great difficulties in phasing the final spectra and therefore allows absolute-value-mode presentation only. In contrast, the CLUB sandwich allows one to obtain high-resolution *phase-sensitive* spectra for many popular 2D PFG experiments, either homonuclear or heteronuclear, by *simply substituting* the CLUB sandwich for a conventional gradient. This is best illustrated by a couple of applications described below.

Application to 2D Spectroscopy

Figure 5 shows the timing diagrams of the phase-sensitive PFG DQF-COSY pulse sequences (*22, 27*) using the CLUB sandwiches. In Fig. 5a we apply two identical decoding CLUB sandwiches which are otherwise exactly the same as the encoding one except possibly different in polarity. This ensures that the ratio of the encoding element to the decoding element is 1:2. An alternative to Fig. 5a is shown in Fig. 5b, in which each individual gradient of the decoding element has been made twice as long as the corresponding gradient in the encoding element. It is essential to refocus the double-quantum evolution during the gradient because it leads to phase shifts that cannot easily be corrected with standard software. Note that the sequences of Figs. 5a and 5b are shown for selection of

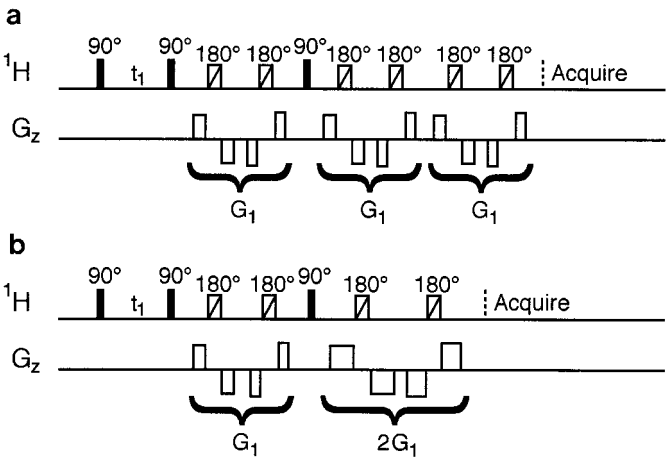

FIG. 5. The timing diagrams of the phase-sensitive PFG DQF-COSY pulse sequences using the CLUB sandwiches. (a) Two identical decoding CLUB sandwiches are applied which are otherwise exactly the same as the encoding CLUB sandwich except possibly different in polarity. (b) An alternative to (a). Each individual gradient of the decoding CLUB sandwich is twice as long as the corresponding gradient in the encoding CLUB sandwich. The scored icons are 60-μs FM pulses using a 25-kHz RF field. The total effective gradient durations we used were 1 and 2 ms for the encoding and decoding elements, respectively.

the coherence transfer pathway $+2 \rightarrow -1$. The other pathway ($-2 \rightarrow -1$) can be selected by simply reversing the polarity of *all* the PFGs in the decoding element. Unlike most PFG experiments, this particular version of the PFG DQF-COSY experiment gives purely amplitude-modulated data sets that can be processed according to standard States–Haberkorn–Ruben procedures (*38*).

The phase-sensitive 2D DQF-COSY spectrum of a crosslinked tripeptide obtained using the pulse sequence of Fig. 5a is shown in the upper panel of Fig. 6. The spectrum shown could be correctly phased without any linear phase correction in either dimension. The lower panel of Fig. 6 shows the expansion of the aromatic region (the dashed square in the upper panel). Most correlations can be identified.

For HSQC (*36*) applications, we need to find a suitably brief and accurate high-power FM pulse which is capable of inverting the entire carbon-13 bandwidth of ca. 25 kHz, or 200 ppm on a 500-MHz spectrometer. Good results were obtained using a 112-μs broadband FM pulse with an RF field of 17.8 kHz, which gives better than 99.5% inversion over the entire protonated carbon-13 chemical shift range (*29*).

Figure 7 shows the timing diagram for the particular PFG version of the HSQC experiment we employed. In order to approximate the first increment to the true $t_1 = 0$ point in the interferometric dimension, an extra delay ϵ is introduced to compensate for evolution during those internal delays for receiver gating and phase setting represented by the delays Δ and the proton 180° pulse time in the middle of t_1. It is well known that a 90° pulse leads to a small linear phase roll (*39*) that can be modeled by an instantaneous δ-function 90° pulse followed by a delay of length $1/\gamma B_1$. If this is also to be included, the delay ϵ can then be set so that

$$\epsilon = 4\Delta + \frac{2}{\gamma B_1} + \tau_{180}, \qquad [10]$$

where τ_{180} is the proton 180° pulse time (excluding any associated hardware delays). While a composite PFG could be used for the decoding gradient G_1, there is little advantage to do so in this particular case, as there is adequate time to apply a strong conventional PFG during the last $1/4J$ delay right before acquisition and still leave adequate time for stabilization. Like most PFG experiments that use gradients to select a particular coherence transfer pathway, the PFG HSQC generates purely phase-modulated data sets which lead to the well-known "phase-twist" lineshape (*40*). For this reason, each t_1 increment has to be repeated with the polarity of either the encoding or the decoding element reversed so that both the "*N*-" and "*P*-type" data sets can be obtained. These are then Fourier transformed with respect to the running time t_2 before they are combined to give the usual purely amplitude-modulated data sets from which the desired double-absorption lineshape can be obtained (*37*, *41*, *42*).

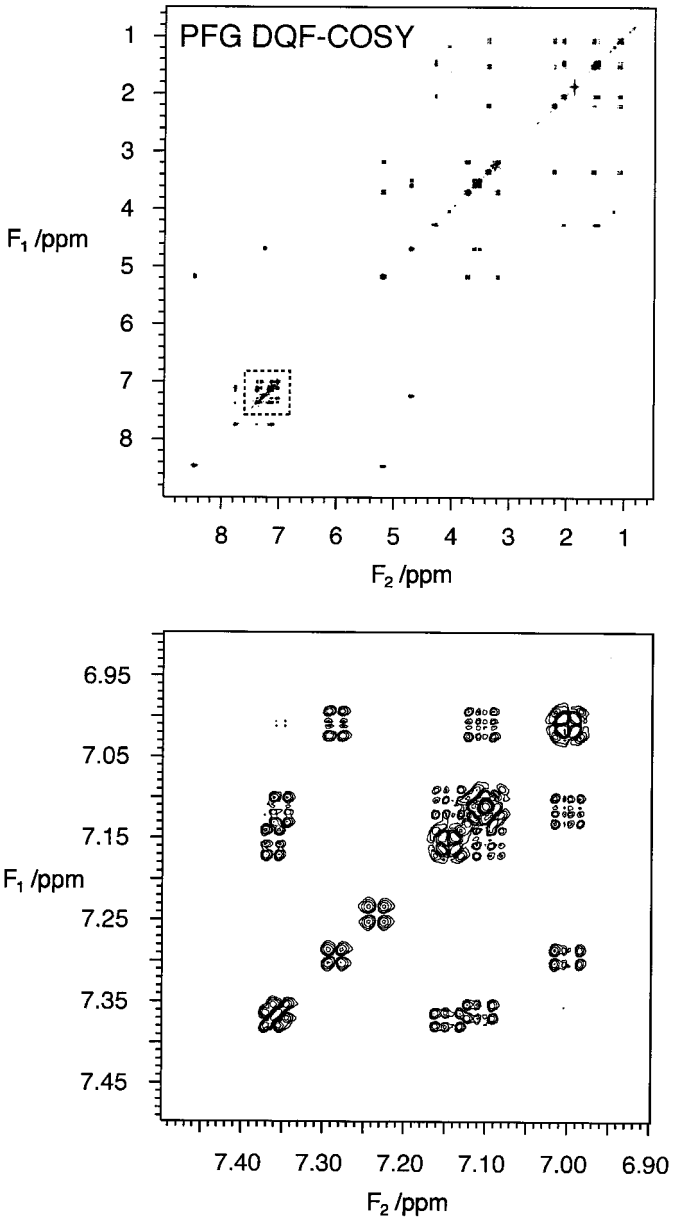

FIG. 6. The phase-sensitive 2D DQF-COSY spectra of the crosslinked tripeptide Ac-Trp-Pro-Trp-OMe in DMSO-d_6 obtained with the pulse sequence of Fig. 5a. The spectral width was 5500 Hz (11 ppm) in both dimensions. Each FID was acquired with two transients and 2048 complex points, zero filled to 4096 points before Fourier transformation. A total of 2048 increments were taken in the t_1 dimension, each repeated with only the phase of the first 90° pulse shifted by 90°. These were then also zero filled to 4096 points. The data were apodized to avoid truncation effects before the standard hypercomplex data processing procedure was carried out. The lower panel shows the expansion of the aromatic region (the dashed square in the upper panel) on a different vertical scale for clarity.

Figure 8 shows the natural abundance 2D HSQC spectrum of the steroid progesterone obtained using the pulse sequence of Fig. 7. A total of 64 t_1 increments were acquired, each repeated with the polarity of the decoding element reversed.

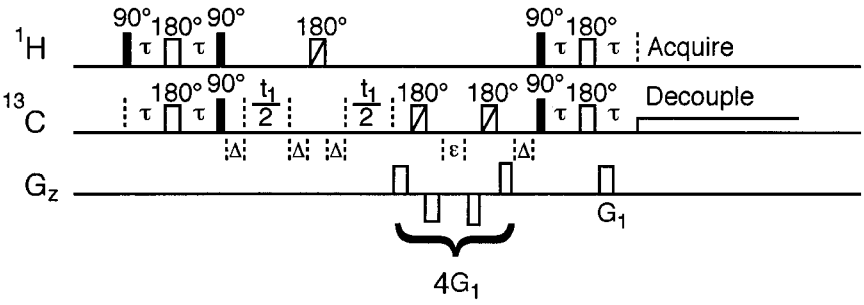

FIG. 7. Pulse sequence timing diagram for the hybrid PFG HSQC experiment. The scored icons are constant-amplitude FM pulses. On the proton channel a 60-μs FM inversion pulse using a 25-kHz RF field was employed, while on the carbon-13 channel these were 112 μs in duration using a 17.8-kHz RF field (*29*). All other 180° pulses represented by open rectangles on the carbon-13 channel are of the type $90^\circ_x 240^\circ_y 90^\circ_x$. With typical internal delays $\Delta = 10$ μs on the proton and carbon-13 pulses and a 14-μs 90° pulsewidth on carbon-13, the compensatory delay ϵ is set to 117.8 μs.

Again near zero linear phase correction was needed in both dimensions. This hybrid PFG version also keeps the suppression ratio extremely high, giving a very clean spectrum free of artifacts.

SUMMARY

In summary, we have proposed a composite pulsed field gradient technique that gives almost instantaneous recovery and refocuses evolution under chemical shift and heteronuclear *J* coupling. While any inversion pulse with arbitrary phase property can be used in this scheme, best results in terms of both suppression and retention were obtained with a family of broadband high-power constant-amplitude FM pulses. Using this new approach we were able to obtain phase-sensitive 2D spectra for both homonuclear and heteronuclear PFG experiments such as DQF-COSY and HSQC with very little effort in phasing the spectra. The success of these applications demonstrates that the CLUB sandwich can simply be substituted for conventional gradients in any pulse sequence when desired. The nucleus-selective nature of this scheme will be the subject of a further investigation.

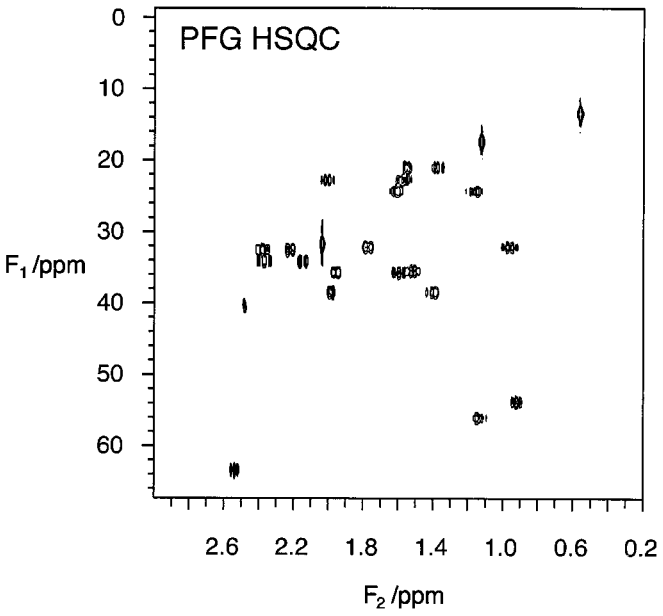

FIG. 8. The phase-sensitive natural abundance HSQC spectrum of the steroid progesterone. The pulse sequence of Fig. 7 was used. The spectrum was obtained with 64 t_1 increments over a spectral width of 8250 Hz (66 ppm), zero filled to 256 points before FT. The spectral width in F_2 was 2000 Hz. Each FID was acquired with four transients and 2048 complex points, zero filled to 4096 points. Each t_1 increment was repeated with only the polarity of the decoding gradient reversed to obtain both *N*- and *P*-type data sets. These were then processed as described in the text to give the final spectrum. Appropriate apodization was applied to avoid large truncation effects.

ACKNOWLEDGMENTS

This material is based on work partially supported by the Dreyfus Foundation and the National Science Foundation, CHE-9625674. We thank Professor David Van Vranken and Mr. Shawn Stachel for making available the crosslinked tripeptide to us.

REFERENCES

1. J. Jeener, B. H. Meier, P. Bachman, and R. R. Ernst, Investigation of exchange processes by two-dimensional NMR spectroscopy, *J. Chem. Phys.* **71,** 4546–4553 (1979).
2. A. Haase, J. Frahm, W. Hanicke, and D. Matthaei, ^{1}H NMR chemical shift selective (CHESS) imaging, *Phys. Med. Biol.* **30,** 341–344 (1985).
3. J. Stonehouse, P. Adell, J. Keeler, and A. J. Shaka, Ultrahigh-quality NOE sepctra, *J. Am. Chem. Soc.* **116,** 6037–6038 (1994).
4. I. M. Brereton, G. J. Galloway, J. Field, M. F. Marshman, and D. M. Doddrell, Gradient-induced water-suppression techniques for high-resolution NMR spectroscopy, *J. Magn. Reson.* **81,** 411–417 (1989).
5. C. T. W. Moonen and P. C. M. van Zijl, Highly effective water suppression for *in vivo* proton NMR spectroscopy (DRYSTEAM), *J. Magn. Reson.* **88,** 28–41 (1990).
6. M. Piotto, V. Saudek, and V. Sklenar, Gradient-tailored excitation for single-quantum NMR spectroscopy, *J. Biomol. NMR* **2,** 661–665 (1992).

7. S. Grzesiek and A. Bax, The importance of not saturating H_2O in protein NMR—Application to sensitivity enhancement and NOE measurements, *J. Am. Chem. Soc.* **115,** 12593–12594 (1993).
8. T. L. Hwang and A. J. Shaka, Water suppression that works—Excitation sculpting using arbitrary waveforms and pulsed field gradients, *J. Magn. Reson. A* **112,** 275–279 (1995).
9. K. Stott, J. Stonehouse, J. Keeler, T. L. Hwang, and A. J. Shaka, Excitation sculpting in high-resolution nuclear magnetic resonance spectroscopy—Application to selective NOE experiments, *J. Am. Chem. Soc.* **117,** 4199–4200 (1995).
10. G. Mackin and A. J. Shaka, Phase-sensitive two-dimensional HMQC and HMQC–TOCSY spectra obtained using double pulsed-field-gradient spin echoes, *J. Magn. Reson. A* **118,** 247–255 (1996).
11. V. V. Krishnamurthy, Phosphorus *J*-scaled band-selective homonuclear-decoupled TOCSY for H3′–^{31}P coupling-constant measurement in DNA oligomers, *J. Magn. Reson. B* **113,** 46–52 (1996).
12. G. Z. Xu and J. S. Evans, The application of excitation sculpting in the construction of selective one-dimensional homonuclear coherence-transfer experiments, *J. Magn. Reson. B* **111,** 183–185 (1996).
13. G. Bodenhausen, R. Freeman, and D. L. Turner, Suppression of artifacts in two-dimensional *J* spectroscopy, *J. Magn. Reson.* **27,** 511–514 (1977).
14. C. J. Turner and S. L. Patt, Artifacts in two-dimensional NMR, *J. Magn. Reson.* **85,** 492–505 (1989).
15. A. E. Derome and M. P. Williamson, Rapid-pulsing artifacts in double-quantum-filtered COSY, *J. Magn. Reson.* **88,** 177–185 (1990).
16. A. Bax and S. S. Pochapsky, Optimized recording of heteronuclear multidimensional NMR spectra using pulsed field gradients, *J. Magn. Reson.* **99,** 638–643 (1992).
17. A. D. Bain, Coherence levels and coherence pathways in NMR, *J. Magn. Reson.* **56,** 418–427 (1984).
18. G. Bodenhausen, H. Kogler, and R. R. Ernst, Selection of coherence-transfer pathways in NMR pulse experiments, *J. Magn. Reson.* **58,** 370–388 (1984).
19. A. A. Maudsley, A. Wokaun, and R. R. Ernst, Coherence transfer echoes, *Chem. Phys. Lett.* **55,** 9–14 (1978).
20. A. Bax, P. G. de Jong, A. F. Mehlkopf, and J. Simdt, Separation of the different orders of NMR multiple-quantum transitions by the use of pulsed field gradients, *Chem. Phys. Lett.* **69,** 567–570 (1980).
21. P. Barker and R. Freeman, Pulsed field gradients in NMR. An alternative to phase cycling, *J. Magn. Reson.* **64,** 334–338 (1985).
22. R. E. Hurd, Gradient-enhanced spectroscopy, *J. Magn. Reson.* **87,** 422–428 (1990).
23. R. E. Hurd and B. K. John, Gradient-enhanced proton-detected heteronuclear multiple-quantum coherence spectroscopy, *J. Magn. Reson.* **91,** 648–653 (1991).
24. A. Wokaun and R. R. Ernst, Selective detection of mutiple quantum transitions in NMR by two-dimensional spectroscopy, *Chem. Phys. Lett.* **52,** 407–412 (1977).
25. U. Piantini, O. W. Sørensen, and R. R. Ernst, Multiple quantum filters for elucidating NMR coupling networks, *J. Am. Chem. Soc.* **104,** 6800–6801 (1982).
26. A. J. Shaka and R. Freeman, Simplification of NMR spectra by filtration through multiple-quantum coherence, *J. Magn. Reson.* **51,** 169–173 (1983).
27. A. L. Davis, E. D. Laue, J. Keeler, D. Moskau, and J. Lohman, Absorption-mode two-dimensional NMR spectra recorded using pulsed field gradients, *J. Magn. Reson.* **94,** 637–644 (1991).
28. B. K. John, D. Plant, P. Webb, and R. E. Hurd, Effective combination of gradients and crafted RF pulses for water suppression in biological samples, *J. Magn. Reson.* **98,** 200–206 (1992).
29. V. A. Mandelshtam, H. Hu, and A. J. Shaka, Two-dimensional HSQC NMR spectra obtained using a self-compensating double pulsed field gradient and processed using the filter diagonalization method, *Magn. Reson. Chem.* **36,** 517–528 (1998).
30. G. Wider, V. Dötsch, and K. Wüthrich, Self-compensating pulsed magnetic-field gradients for short recovery times, *J. Magn. Reson. A* **108,** 255–258 (1994).
31. V. Dötsch, G. Wider, and K. Wüthrich, Phase-sensitive spectra in a single scan with coherence selection by pulsed field gradients, *J. Magn. Reson. A* **109,** 263–264 (1994).
32. D. H. Wu and C. S. Johnson, Radiation-damping effects on relaxation-time measurements by the inversion-recovery method, *J. Magn. Reson. A* **110,** 113–117 (1994).
33. K. J. Packer and K. M. Wright, The use of single-spin operator basis sets in the NMR spectroscopy of scalar-coupled spin systems, *Mol. Phys.* **50,** 797–813 (1983).
34. O. W. Sørensen, G. W. Eich, M. H. Levitt, G. Bodenhausen, and R. R. Ernst, Product operator formalism for the description of NMR pulse experiments, *Prog. NMR Spectrosc.* **16,** 163–192 (1983).
35. A. J. Shaka and R. Freeman, A composite 180° pulse for spatial localization, *J. Magn. Reson.* **63,** 596–600 (1985).
36. G. Bodenhausen and D. J. Ruben, Natural abundance nitrogen-15 NMR by enhanced heteronuclear spectroscopy, *Chem. Phys. Lett.* **69,** 185–189 (1980).
37. A. L. Davis, J. Keeler, E. D. Laue, and D. Moskau, Experiments for recording pure-absorption heteronuclear correlation spectra using pulsed field gradients, *J. Magn. Reson.* **98,** 207–216 (1992).
38. D. J. States, R. A. Haberkorn, and D. J. Ruben, A two-dimensional nuclear Overhauser experiment with pure absorption phase in four quadrants, *J. Magn. Reson.* **48,** 286–292 (1982).
39. R. R. Ernst, G. Bodenhausen, and A. Wokaun, "Principles of Nuclear Magnetic Resonance in One and Two dimensions," pp. 119–122, Clarendon Press, Oxford (1997).
40. G. Bodenhausen, R. Freeman, R. Niedermeyer, and D. L. Turner, Double Fourier transformation in high-resolution NMR, *J. Magn. Reson.* **26,** 133–164 (1977).
41. J. Keeler and D. Neuhaus, Comparison and evaluation of methods for two-dimensional NMR spectra with absorption-mode lineshapes, *J. Magn. Reson.* **63,** 454–472 (1985).
42. J. R. Tolman, J. Chung, and J. H. Prestegard, Pure-phase heteronuclear multiple-quantum spectroscopy using field gradient selection, *J. Magn. Reson.* **98,** 462–467 (1992).